

# 550-mW Output Power From a Narrow Linewidth All-Phosphate Fiber Laser

Peter Hofmann, Christian Voigtländer, Stefan Nolte, N. Peyghambarian, and Axel Schülzgen

**Abstract**—We present a compact monolithic all-phosphate glass fiber laser with up to 550 mW of output power operating on a single longitudinal mode. We measured a linewidth of less than 60 kHz and relaxation oscillation peak amplitudes below  $-100$  dB/Hz without active RIN-suppression. The laser cavity has been formed by inscribing fiber Bragg gratings (FBG) directly into heavily  $\text{Er}^{3+}\text{Yb}^{3+}$  doped phosphate glass fiber using femtosecond laser pulses and a phasemask. The compact form factor and higher output power combined with the low noise and narrow line width characteristic make this laser an ideal candidate for ranging, interferometry and sensing applications.

**Index Terms**—Fiber Bragg grating (FBG), optical fiber fabrication, photosensitivity, photo thermo refractive glass.

## I. INTRODUCTION

**P**OWER scalability, narrow linewidth, and a resulting large coherence length makes single frequency fiber lasers desirable light sources in sensing, ranging, interferometry, and high-resolution spectroscopy applications. To date, single frequency fiber lasers have been implemented as distributed feedback (DFB) fiber lasers [1], short-cavity distributed Bragg reflector (DBR) fiber lasers [2], ring cavity fiber lasers with narrow-bandwidth spectral filters [3], [4], Brillouin fiber lasers [5], and injection-locked fiber lasers [6]. Although being known for having relatively limited output power, DFB and short-length linear cavity DBR lasers are particularly attractive due to their compactness, simplicity, and robustness. A common approach for achieving higher output power single-frequency sources is the amplification of a seed laser by one or more  $\text{Er}^{3+}\text{Yb}^{3+}$  fiber amplifier stages to reach watt levels. Disadvantages of this method include increased complexity and noise amplification, making it difficult to reach the quantum noise level. Recently, highly  $\text{Er}^{3+}\text{Yb}^{3+}$  doped phosphate glass fibers have been developed and successfully

used to implement compact narrow-linewidth linear cavity fiber lasers with improved output power [7], [8].

Phosphate glass is well known for its superior cluster-free rare earth ion solubility [9]. Doping concentrations of several wt% have been reached, resulting in large gain per unit length, and making ultracompact laser devices with high output power possible [10]. When compared with other nonsilica based fibers, phosphate glass fibers also exhibit relatively low attenuation due to scattering of the order of  $1.5 \text{ m}^{-1}$  [11], as well as reasonable mechanical strength. The highest power from a short-linear-cavity single-frequency phosphate glass fiber laser in the C-band reported to date is 300 mW using a 2-cm section of highly doped  $\text{Er}^{3+}\text{Yb}^{3+}$  phosphate glass fiber spliced to a conventional FBG serving as an output coupler [12]. It is worth noting that, in this work, the researchers used a dielectric mirror as a high reflector, so it is strictly speaking not an all-fiber device.

Although splicing conventional silica-based FBGs to  $\text{Er}^{3+}\text{Yb}^{3+}$  doped phosphate glass fiber is a common technique to fabricate phosphate glass fiber lasers, these “hybrid” devices have obvious shortcomings. First, due to their largely different physical properties, splicing of phosphate glass fibers to silica fibers is challenging. The resulting splice joints exhibit significantly reduced mechanical strength and relatively high optical losses of about 0.5 dB/splice, both of which is undesirable inside a laser cavity. Second, the active region in a hybrid laser is always shorter than the effective cavity length. This is due to the fact that for manufacturing reasons, the fusion splice is about 1 cm displaced from the FBG. In addition, the electric field that is penetrating into the FBG does not experience gain either. In a linear cavity fiber laser, where the effective cavity length is limited to a few centimeters to ensure stable single-mode operation, this can easily mean a 50% reduction of the length of the active region, therefore limiting the output power of the laser for a given effective cavity length.

In contrast, a monolithic laser design can overcome these shortcomings altogether, in particular if the FBGs are written directly into the active fiber, having the advantage that the whole effective cavity length also is available for amplification. Another advantage is that any splices are removed from inside the cavity, reducing the cavity round-trip loss and therefore reducing the laser threshold.

Unfortunately, phosphate glass is lacking inherent photosensitivity, which makes it challenging to write FBGs directly into these fibers. Moreover, traditional methods of photo-sensitization have not been very successful in phosphate glass [13], [14]. A more promising method is UV inscription of Type-II gratings at 193 nm wavelength [15], which may be combined with

Manuscript received August 31, 2012; revised October 22, 2012; accepted December 03, 2012. Date of publication December 11, 2012; date of current version January 23, 2013. This work was supported by the Center for Integrated Access Networks (CIAN) at the University of Arizona.

P. Hofmann and N. Peyghambarian are with the College of Optical Sciences, University of Arizona, Tucson, AZ 30332 USA (e-mail: phofmann@optics.arizona.edu; nnp@optics.arizona.edu).

C. Voigtländer and S. Nolte are with the Institute of Applied Physics, Abbe Center of Photonics, Friedrich-Schiller-University Jena, 07743 Jena, Germany (e-mail: ch.voigtlaender@uni-jena.de; stefan.nolte@uni-jena.de).

A. Schülzgen is with CREOL, The College of Optics and Photonics, University of Central Florida, Orlando, FL 32816 USA (e-mail: axel@creol.ucf.edu).

Color versions of one or more of the figures in this paper are available online at <http://ieeexplore.ieee.org>.

Digital Object Identifier 10.1109/JLT.2012.2233392

subsequent photothermal growth [16] to enhance the grating's final reflectivity. We previously reported an all phosphate glass monolithic fiber laser [17] where we used an intense UV beam from a pulsed 193-nm ArF excimer laser to inscribe the gratings directly into the active fiber. However, with this writing method, we observed relatively large scattering losses [18] in the FBG. Lower scattering losses have been achieved using IR-femtosecond pulses instead of the UV wavelength, first reported in [19] and shortly thereafter in phosphate glass fibers [20], but, to the best of our knowledge, have not yet been utilized to build monolithic phosphate fiber lasers.

## II. EXPERIMENTS

Here, we demonstrate a compact monolithic phosphate glass fiber laser with 550 mW of stable output power. The oscillator power was reached by utilizing powerful multimode pump diodes and a cladding pumping scheme. Similar cladding pumped techniques have been used recently to demonstrate watt-level compact fiber lasers with the hybrid phosphate-silica approach [21]–[23]. However, these early attempts have suffered from random bursts of sustained self-pulsing (SSP), making it impossible to measure laser intensity noise or linewidth.

SSP is the periodic emission of laser pulses at a repetition rate that can be associated to relaxation oscillations [24]. In general, it is observed within a particular pumping range and is enhanced by a low cavity photon lifetime [24]. After a laser has reached its steady state, SSP may occur when the laser is suddenly perturbed by small fluctuations in gain, cavity loss or cavity alignment [25]. Since the temperature sensitivity of a FBGs reflection spectrum is well known, accurate control of the FBGs temperature is one way to reduce SSP.

We therefore combined our all-phosphate fiber laser design with improved packaging and grating temperature stabilization to  $\pm 0.01$  °C. The two closely spaced FBGs have been directly inscribed into the core of a homemade single mode phosphate glass fiber. The fiber had a core diameter of  $2a = 11$   $\mu\text{m}$ , a cladding diameter of 125  $\mu\text{m}$ , and a doping of 1 wt%  $\text{Er}_2\text{O}_3$  and 8 wt%  $\text{Yb}_2\text{O}_3$  in the core. The fiber's two dimensional refractive index profile was measured over a wavelength range from 550 to 1080 nm using an interferometric fiber profilometer (Interfiber Analysis, Inc.; IFA-100). Cross sections of the refractive index profiles for three selected wavelengths are plotted in Fig. 1(a), clearly showing the step index profile resulting from the rod-in-tube fiber fabrication process. From the measured refractive index profiles, the wavelength dependence of the fiber's core and cladding refractive index has been obtained as shown in Fig. 1(b). The measurement results have then been fitted to the well-known Sellmeier equation. The fits are also plotted in Fig. 1(b) (solid lines). The refractive index difference between core and cladding  $\Delta n$  was obtained by subtracting the two dispersion curves.  $\Delta n$  was almost constant over the measured wavelength range (Fig. 1(b) dashed-dot right  $y$ -axis). The fiber's NA in the weak guidance approximation [26] is given by

$$\text{NA} = n_{\text{core}} \sqrt{2\Delta} \quad (1)$$

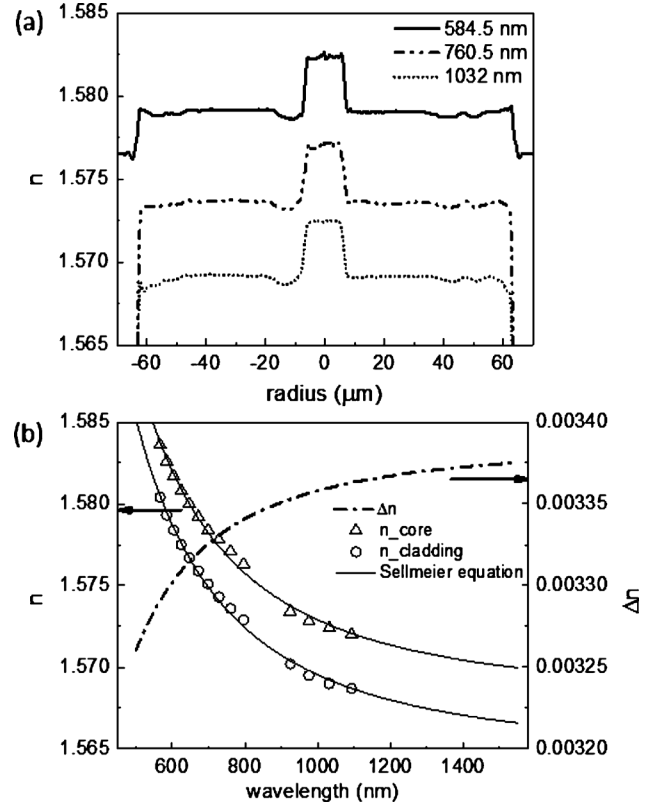


Fig. 1. (a) Measured refractive index profiles of the homemade phosphate fiber at selected wavelengths. (b) Plotted as a function of wavelength are: the measured refractive index of the phosphate fiber's core (triangles) and cladding (circles), along with the Sellmeier fit (all on left  $y$ -axis) and  $\Delta n$  (right  $y$ -axis).

where  $\Delta = n_{\text{core}}/n_{\text{clad}} - 1$  is the relative refractive index difference. At a wavelength of 1550 nm, the NA is consequently  $0.103 \pm 0.005$ . Using again the weak guidance approximation [26], the single mode cutoff wavelength of the phosphate fiber can be calculated as

$$\lambda_c = \frac{2\pi n_{\text{core}} a}{2.405} \sqrt{2\Delta} \quad (2)$$

indicating that the fiber supports only the fundamental transverse mode (LP<sub>01</sub>) at the lasing wavelength of 1538 nm. Two FBGs were inscribed into this fiber using the phase mask scanning technique [27]. The ultrafast laser used for the inscription process is a commercial Ti:sapphire CPA system with a pulse energy of 1 mJ, a repetition rate of 1 kHz, and a pulse duration of 150 fs. The laser beam was focused by a 20-mm cylindrical lens through the phase mask (period of  $\Lambda = 1.965$   $\mu\text{m}$ ) into the fiber core. By moving fiber and phase mask underneath the laser beam, the FBGs could be elongated. A measurement performed with an optical backscatter reflectometer (Lunatech, Inc.; OBR4400) shows the FBGs inside the phosphate glass fiber. Here the high reflector (HR) grating has a length of 12 mm, the low reflector (LR) grating is 8 mm long and the spacing between the two gratings is approximately 60 mm [Fig. 2(a)]. Shown in Fig. 2(b) is a transmission spectrum of the fiber laser cavity where the LR has been intentionally shifted by heating. The reflectivities of the LR and HR were 60% and 94%, respectively. This monolithic fiber laser cavity has then been fusion spliced on both ends to commercial double clad fiber (Coractive

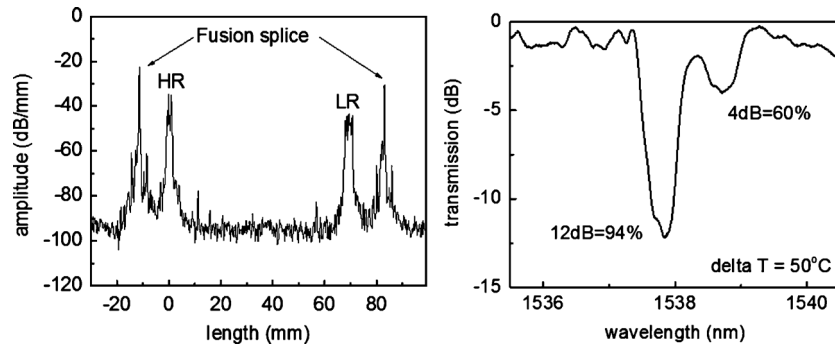


Fig. 2. (a) Measurement trace from optical backscatter reflectometer showing the position of the fusion splices and the FBGs within the phosphate glass fiber. The distance between the two gratings is approximately 60 mm. (b) Transmission spectra through a pair of intentionally temperature-detuned femtosecond-written FBGs.

DCF-UN-8/125-14) using a specially developed splice recipe on a conventional fusion splicer (Ericsson, Inc.; FSU995PM). The fiber chain was then placed on a V-grooved microscope slide. To ensure optical confinement of the pump light, the fiber cladding has been recoated with a UV-curable low index polymer (Efiron UVF PC373-AP). Microscope cover slides were used to complete the encapsulation of the fiber chain. This packaging ensures high mechanical stability and still allows for efficient heat removal using two 4-W thermo-electric coolers. To characterize the performance of the phosphate glass laser, an experimental setup, which is shown schematically in Fig. 3(a), has been used. A diode laser module operating at a wavelength of 975 nm (LIMO, Inc.) with a spectral bandwidth of  $\approx 3$  nm and a maximum output power of up to 35 W is fiber coupled to a multimode fiber with 105- $\mu\text{m}$  core diameter and a numerical aperture of 0.22. The multimode pump fiber was fusion spliced to one pump port of a multi-mode 2 + 1 pump and signal combiner (ITFlabs, Inc.; MMC02112CC1). The output port of the combiner was fusion spliced to the LR side of the phosphate glass laser. The signal port of the combiner was used to collect the laser's output signal and has been fed through an optical isolator to reduce back reflections into the laser cavity. A 1  $\times$  4 signal splitter (not shown here) was used to divide the laser output to simultaneously perform further analysis.

One port was connected to an optical spectrum analyzer (OSA). The trace from the OSA is shown in Fig. 3(a). The lasing wavelength was 1538.2 nm and the side mode suppression ratio was 72 dB.

An optical power meter was used to measure the laser output power as a function of absorbed pump power. The results are plotted in Fig. 3(c). The lasing threshold was found to be at 200-mW pump power. The laser reached a maximum output power of 550 mW and maintained a slope efficiency of 12% throughout the pumping range. During a 60 min measurement interval the output power did not fluctuate by more than  $\pm 0.4\%$ .

For laser intensity noise measurements, a fast photodetector (FPD) with a bandwidth of 12 GHz and a responsivity of 0.6 A/W was used. The photodetector signal was amplified using a low noise amplifier with a bandwidth of 1 GHz and a gain of 50 dB. The amplified signal was then fed into an electrical spectrum analyzer (Agilent E4403B).

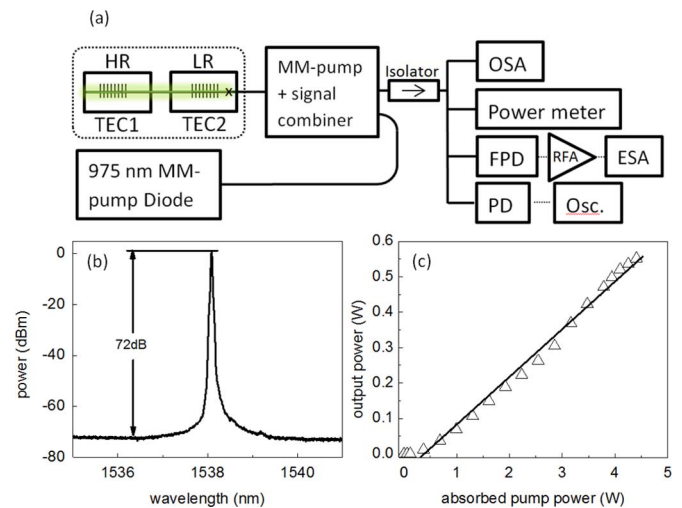


Fig. 3. (a) Experimental setup used to characterize the monolithic phosphate glass fiber lasers. (b) Measurement trace from the optical spectrum analyzer. The laser shows a side-mode suppression ratio of 72 dB. The resolution bandwidth of the OSA was 20 pm. (c) Laser output power versus absorbed pump power. The slope efficiency was 12%.

A second photodetector, which was connected to an oscilloscope, was used to confirm that the laser was not showing sustained self pulsation at the relaxation oscillation frequency or any other transient behavior. By carefully adjusting the temperature of the gratings it was possible to operate the laser at a single longitudinal mode, stable enough to analyze the emission with an electrical spectrum analyzer (ESA) and measuring relative intensity noise (RIN) spectra.

In order to measure the linewidth and short term wavelength drift of the laser, an optical heterodyne and an optical delayed-self heterodyne analysis have been performed. Detailed descriptions of both measurement methods are provided in [28]. For the optical heterodyne measurement an Agilent 81640A tunable laser source with a linewidth of  $< 100$  kHz was used as a local oscillator and a 3-dB coupler to mix the signal of the phosphate glass fiber laser with the local oscillator (setup is not shown here). The interference was then detected with the previously described fast photodiode and the ESA was used to record the electrical power spectrum. Fig. 4(a) shows the heterodyne beat

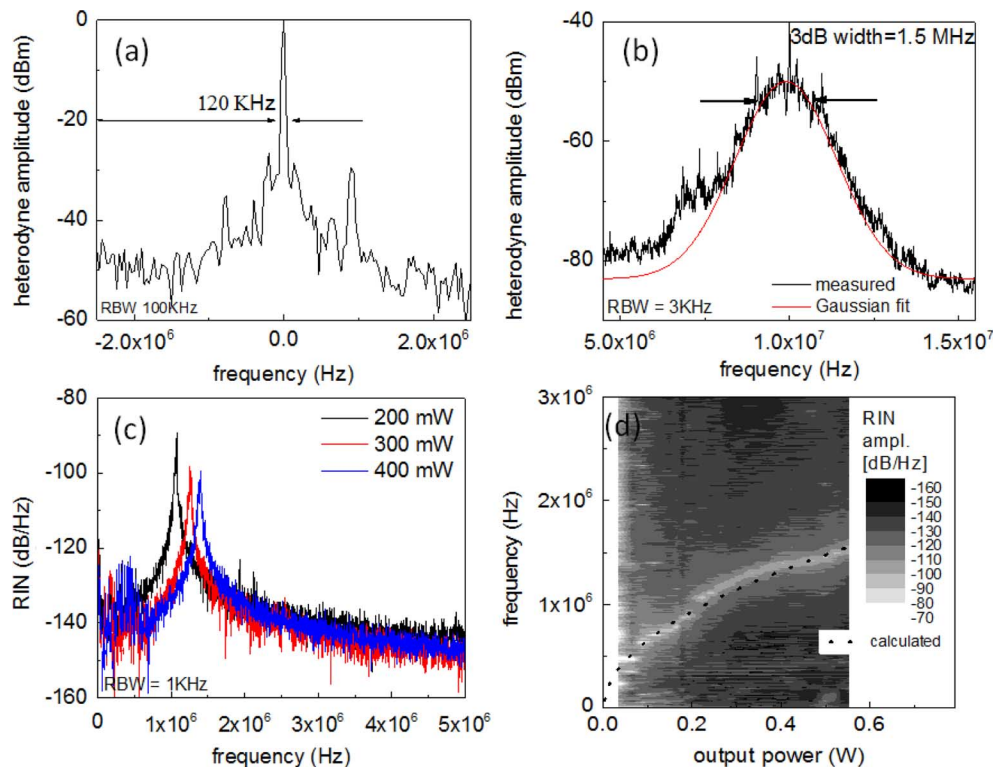


Fig. 4. (a) Single-shot heterodyne spectrum. (b) Time-averaged self-delayed heterodyne spectrum. (c) RIN spectra at selected output power levels. (d) Relaxation oscillation peak frequency versus laser output power.

signal. The width of the spectrum is limited by the linewidth of the Agilent laser. We estimate the linewidth of our phosphate glass laser to be less than 60 kHz.

To measure the short-term wavelength drift, we used a self-delayed heterodyne setup with 25 km of smf28 fiber serving as delay line and increased the integration time of the ESA to 3 s. As it can be seen in Fig. 4(b), time averaging of the self-delayed heterodyne spectrum results in a broadened spectrum with a 3-dB bandwidth of 1.5 MHz, which can be attributed to a short-term laser wavelength drift. As a consequence, applications requiring an increased measurement time or delay length essentially will see a reduced coherence length from the laser. The reduction of this drift is currently subject of our research.

Last, the all-phosphate glass fiber laser's RIN spectra were measured from 1 kHz to 5 MHz. The ESA was operating at a resolution bandwidth of 10 kHz. The spectra are shown in Fig. 4(c). Each spectrum is dominated by a characteristic peak at the relaxation oscillation frequency around 1 MHz. The noise decreases then monotonically towards higher frequencies. As the laser output power increases, the RIN peak shifts towards higher frequencies. As it is expected from textbook analysis, Fig. 4(d) confirms that the frequency shift of the RIN peak follows in good approximation the square root of the laser output power.

### III. CONCLUSION

We have demonstrated a monolithic single-frequency cladding pumped phosphate glass fiber laser with stable high output power and low-intensity noise. This device overcomes the stability problems [21]–[23] and power limitations [8], [17]

of previous phosphate glass fiber lasers. The fact that multimode pump diodes are readily available at a much lower cost along with the high rare-earth solubility of phosphate glass fibers makes this approach an ideal candidate for power scalability of low-noise compact single-frequency fiber lasers and therefore a promising competitor for MOPA configurations. In the future, we are seeking to further reduce the linewidth, improve the single-mode robustness of our laser by developing gratings with a narrower linewidth, and develop a large mode-area fiber to further increase the output power.

### REFERENCES

- [1] M. Sejka, P. Varming, J. Hubner, and M. Kristensen, "Distributed feedback Er<sup>3+</sup>-doped fibre laser," *Electron. Lett.*, vol. 31, no. 17, pp. 1445–1446, 1995.
- [2] G. A. Ball, W. W. Morey, and W. H. Glenn, "Standing wave monomode erbium fiber laser," *IEEE Photon. Technol. Lett.*, vol. 3, no. 7, pp. 613–615, Jul. 1991.
- [3] K. Iwatsuki, H. Okamura, and M. Saruwatari, "Wavelength-tunable single-frequency and single-polarisation Er-doped fibre ring-laser with 1.4 kHz linewidth," *Electron. Lett.*, vol. 26, no. 24, pp. 2033–2034, 1990.
- [4] A. Polynkin, P. Polynkin, M. Mansuripur, and N. Peyghambarian, "Single-frequency fiber ring laser with 1 W output power at 1.5  $\mu\text{m}$ ," *Opt. Exp.*, vol. 13, no. 8, pp. 3179–3186, 2005.
- [5] S. P. Smith, F. Zarinetchi, and S. Ezekiel, "Narrow-linewidth stimulated Brillouin fiber laser and applications," *Opt. Lett.*, vol. 16, no. 6, pp. 393–395, 1991.
- [6] X. Zhang, N. H. Zhu, L. Xie, and B. X. Feng, "A stabilized and tunable single-frequency erbium-doped fiber ring laser employing external injection locking," *J. Lightw. Technol.*, vol. 25, no. 4, pp. 1027–1033, Apr. 2007.
- [7] J. D. Myers, R. Wu, T. L. Chen, M. Myers, C. R. Hardy, and J. K. Driver, "Phosphate glass fiber laser materials and architectures," in *Proc. Annu. Solid State and Diode Laser Technol. Rev.*, Los Angeles, CA, 2003.

- [8] C. Spiegelberg, J. Geng, Y. Hu, Y. Kaneda, S. Jiang, and N. Peyghambarian, "Low-noise narrow-linewidth fiber laser at 1550 nm," *J. Lightw. Technol.*, vol. 22, no. 1, pp. 57–62, Jan. 2004.
- [9] K. Seneschal, F. Smektala, B. Bureau, M. Le Floch, S. Jiang, T. Luo, J. Lucas, and N. Peyghambarian, "Properties and structure of high erbium doped phosphate glass for short optical fibers amplifiers," *Mater. Res. Bull.*, vol. 40, no. 9, pp. 1433–1442, 2005.
- [10] T. Qiu, L. Li, A. Schülzgen, V. L. Temyanko, T. Luo, S. Jiang, A. Mafi, J. V. Moloney, and N. Peyghambarian, "Generation of 9.3-W multimode and 4-W single-mode output from 7-cm short fiber lasers," *IEEE Photon. Technol. Lett.*, vol. 16, no. 12, pp. 2592–2594, Dec. 2004.
- [11] L. Li, M. M. Morrell, T. Qiu, V. L. Temyanko, A. Schülzgen, A. Mafi, D. Kuznetsov, J. V. Moloney, T. Luo, S. Jiang, and N. Peyghambarian, "Short cladding-pumped Er/Yb phosphate fiber laser with 1.5 W output power," *Appl. Phys. Lett.*, vol. 85, no. 14, pp. 2721–2723, 2004.
- [12] S. H. Xu, Z. M. Yang, T. Liu, W. N. Zhang, Z. M. Feng, Q. Y. Zhang, and Z. H. Jiang, "An efficient compact 300 mW narrow-linewidth single frequency fiber laser at 1.5  $\mu\text{m}$ ," *Opt. Exp.*, vol. 22, no. 2, pp. 1249–1254, 2010.
- [13] S. Pissadakis, A. Ikiades, P. Hua, A. K. Sheridan, and J. S. Wilkinson, "Photosensitivity of ion-exchanged Er-doped phosphate glass using 248 nm excimer laser radiation," *Opt. Exp.*, vol. 12, no. 14, pp. 3131–3136, 2004.
- [14] S. Suzuki, A. Schülzgen, S. Sabet, J. V. Moloney, and N. Peyghambarian, "Photosensitivity of Ge-doped phosphate glass to 244 nm irradiation," *Appl. Phys. Lett.*, vol. 89, 2006, Art. ID 171913.
- [15] J. Albert, A. Schülzgen, V. L. Temyanko, S. Honkanen, and N. Peyghambarian, "Strong Bragg gratings in phosphate glass single mode fiber," *Appl. Phys. Lett.*, vol. 89, 2006, Art. ID 101127.
- [16] R. M. Rogojan, A. Schülzgen, N. Peyghambarian, A. Laronche, and J. Albert, "Bragg gratings, photosensitivity, and poling in glass waveguides," in *OSA Tech. Dig.*, 2007, Paper BTuC3.
- [17] L. Xiong, P. Hofmann, A. Schülzgen, N. Peyghambarian, and J. Albert, "A short dual-wavelength DBR phosphate fiber laser," in *Proc. CLEO: Laser Applications to Photonic Applications*, 2011.
- [18] P. Hofmann, A. Pirson-Chavez, A. Schülzgen, L. Xiong, A. Laronche, J. Albert, and N. Peyghambarian, "Low noise single frequency all-phosphate fiber laser," in *Proc. SPIE*, 2011, vol. 8039, Art. ID 803911.
- [19] S. J. Mihailov, C. W. Smelser, D. Grobnic, R. B. Walker, P. Lu, H. Ding, and J. Unruh, "Bragg gratings written in all-SiO<sub>2</sub> and Ge-doped core fibers with 800-nm femtosecond radiation and a phase mask," *J. Lightw. Tech.*, vol. 22, no. 1, pp. 943–945, Jan. 2004.
- [20] D. Grobnic, S. J. Mihailov, R. B. Walker, C. W. Smelser, C. Lafond, and A. Croteau, "Bragg gratings made with a femtosecond laser in heavily doped ErYb phosphate glass fiber," *IEEE Photon. Technol. Lett.*, vol. 19, no. 12, pp. 943–945, Jun. 2007.
- [21] T. Qiu, A. Schülzgen, L. Li, A. Polynkin, V. L. Temyanko, J. V. Moloney, and N. Peyghambarian, "Generation of watt-level single-longitudinal-mode output from cladding-pumped short fiber lasers," *Opt. Lett.*, vol. 30, no. 20, pp. 2748–2750, Oct. 15, 2005.
- [22] A. Schülzgen, L. Li, V. L. Temyanko, S. Suzuki, J. V. Moloney, and N. Peyghambarian, "Single-frequency fiber oscillator with watt-level output power using photonic crystal phosphate glass fiber," *Opt. Exp.*, vol. 14, no. 16, pp. 7087–7092, Aug. 07, 2006.
- [23] L. Li, A. Schülzgen, V. L. Temyanko, M. M. Morrell, S. Sabet, H. Li, J. V. Moloney, and N. Peyghambarian, "Ultrapact cladding-pumped 35-mm-short fiber laser with 4.7-W singlemode output power," *Appl. Phys. Lett.*, vol. 88, 2006, Art. ID 161106.
- [24] F. Brunet, Y. Taillon, P. Galarneau, and S. LaRochelle, "A simple model describing both self-mode locking and sustained self-pulsing in ytterbium-doped ring fiber lasers," *J. Lightw. Technol.*, vol. 23, no. 6, pp. 2131–2138, Jun. 2005.
- [25] A. E. Siegman, *Lasers*. Sausalito, CA: University Science, 1986, sec. 25.1.
- [26] D. Gloge, "Weakly guiding fibers," *Appl. Opt.*, vol. 10, no. 10, pp. 2252–2258, Oct. 1971.
- [27] J. Thomas, E. Wikszak, T. Clausnitzer, U. Fuchs, U. Zeitner, S. Nolte, and A. Tünnermann, "Inscription of fiber Bragg gratings with femtosecond pulses using a phase mask scanning technique," *Appl. Phys. A*, vol. 86, pp. 153–157, 2007.
- [28] D. Derickson, *Fiber Optic Test and Measurement*. Upper Saddle River, NJ: Hewlett-Packard Professional Books, 1998, sec. 5.3.